Theoretical and Experimental Studies of Hydride Addition to Iron Carbonyl Phosphine and Phosphite Complexes

David A. Brown,* John P. Deignan, Noel J. Fitzpatrick,* Geraldine M. Fitzpatrick, and William K. Glass*

Department of Chemistry, University College, Belfield, Dublin 4, Ireland

Received November 15, 2000

The hybrid density functional B3LYP method has been used to study the reactions of the organometallic cations $[(\eta^5\text{-}C_5H_5)Fe(CO)_2(PR_3)]^+$ (R = H (**1**), OMe (**8**)) with the hydride anion H^-. From a comparison of the relative energies of the 14 stationary points located on both potential energy surfaces, it was predicted that the most energetically favorable sites of attack would be to one of the CO ligands leading to the formyl species $(\eta^5\text{-}C_5H_5)Fe(CHO)(CO)(PR_3)$ (R = H (**4**), OMe (**10**)) and to the cyclopentadienyl ring leading to the ring adducts $(\eta^4\text{-}C_5H_6)Fe(CO)_2(PR_3)$ (R = H (**7**), OMe (**12**)). Two metallophosphoranes, $(\eta^5\text{-}C_5H_5)Fe(CO)_2(PR_3H)$ (R = H (**2**), OMe (**9**)), resulting from attack to the coordinated phosphorus atom, were located and were found to be significantly less stable than the formyl species or the ring adducts. The hydride species $(\eta^5\text{-}C_5H_5)Fe(CO)_2(H)$ (**5**) and $(\eta^5\text{-}C_5H_5)Fe(CO)(H)(PR_3)$ (R = H (**6**), OMe (**11**)) were located, and since the relative energies of these species were below those of the formyls **4** and **10**, it was predicted that once these formyl species are formed they can undergo loss of the carbonyl, phosphine, or phosphite ligands to give the respective hydrides. In addition, two transition states, **TS1** and **TS2**, for decomposition of the formyl species **4** to the hydride **5** or **6** were located. Since the relative energies of **TS1** and **TS2** were found to be similar, it was predicted that both hydrides would be formed from **4**. These predictions agreed with the experimental evidence obtained from the reduction of the mononuclear cations $[(\eta^5\text{-}C_5H_5)Fe(CO)_2(PR_3)]BF_4$ (R = OMe (**8a**), OEt (**13**)).

Introduction

The reactions of nucleophiles with π-acid metal complexes, (polyene)ML_n, have been studied extensively by exploring the role of the nucleophile,[1−3] the substrate,[4,5] the ligands L,[6,7] and the solvent.[8−10] In principle, a variety of products may form following metal−ring fission, including ring adducts, carbonyl substitution and addition products, and substituted metal carbonyls. The formation of ring adducts (generally with *exo* conformation) and subsequent removal of the ML_n group gives in the case of carbanion nucleophiles substituted ring products containing a new C−C bond, and this reaction is of considerable synthetic value.[11,12]

Theoretical attempts to understand and predict the site of initial attack by a nucleophile on a (polyene)-ML_n system have met with varying degrees of success. Calculations of the interaction energies between quite large nucleophiles such as phosphines and phosphites with a series of tricarbonyl(η^6-arene)manganese cations gave a good correlation with experiment,[13] and a similar approach by Weber and co-workers was applied successfully to the addition of a carbanion to $(\eta^6\text{-}C_6H_6)Cr(CO)_3$.[14]

For such large nucleophiles, the use of ab initio methods to calculate the energies of various intermediates and related activation energies is still difficult and computationally expensive. However, for the simple monatomic hydride anion, H^-, ab initio calculations are practicable; for example, in the case of hydride attack on $[(\eta^5\text{-}C_5H_5)Fe(CO)_3]^+$ ab initio MO results correlated well with low-temperature spectroscopic studies.[15]

In the present paper, the reaction between hydride, H^-, and $[(\eta^5\text{-}C_5H_5)Fe(CO)_2(PH_3)]^+$ (**1**) and $[(\eta^5\text{-}C_5H_5)Fe$-

(1) Kane-Maguire, L. A. P.; Honig, E. D.; Sweigart, D. A. *Chem. Rev.* **1984**, *84*, 525.
(2) Coville, N. J.; Darling, E. A.; Hearn, A. W.; Johnston, P. *J. Organomet. Chem.* **1987**, *328*, 375.
(3) Nakazawa, H.; Kubo, K.; Miyoshi, K. *J. Am. Chem. Soc.* **1983**, *115*, 5863.
(4) Davies, S. G.; Hibberd, J.; Simpson, S. J. Thomas, S. E.; Watts, O. *J. Chem. Soc., Dalton Trans.* **1984**, 701.
(5) Cameron, A. D.; Laycock, D. E.; Smith, V. H., Jr.; Baird, M. C. *J. Chem. Soc., Dalton Trans.* **1987**, 2857.
(6) Atton, J. G.; Kane-Maguire, L. A. P. *J. Organomet. Chem.* **1982**, *226*, C43.
(7) Lapinte, C.; Catheline, D.; Astruc, D. *Organometallics* **1984**, *3*, 817.
(8) Brown, D. A.; Chawla, S. K.; Glass, W. K.; Hussein, F. A. *Inorg. Chem.* **1982**, *21*, 2726.
(9) Davies, S. G.; Hibberd, J.; Simpson, S. J. *J. Organomet. Chem.* **1983**, *246*, C16.
(10) Morken, A. M.; Eyman, D. P.; Wolff, M. A.; Schauer, S. J. *Organometallics* **1993**, *12*, 725.
(11) Semmelhack, M. F. In *Organic Synthesis: Today, Tomorrow*; Trost, B. M., Hutchinson, C. R., Eds.; 3rd IUPAC Symposium on Organic Synthesis; Pergamon: Oxford, U.K., 1981; p 63.
(12) Pearson, A. J. *J. Compr. Org. Synth.* **1991**, *4*, 663.
(13) Brown, D. A.; Burns, J. C.; Conlon, P. A.; Deignan, J. P.; Fitzpatrick, N. J.; Glass, W. K.; O'Byrne, P. *Organometallics* **1996**, *15*, 3147.
(14) Weber, J.; Morgantini, P. Y.; Eisenstein, O. *J. Mol. Struct. (THEOCHEM)* **1992**, *254*, 343.
(15) Brown, D. A.; Fitzpatrick, N. J.; Groarke, P. J.; Koga, K.; Morokuma, K. *Organometallics* **1993**, *12*, 2521.

10.1021/om0009740 CCC: $20.00
Publication on Web 03/23/2001

$(CO)_2\{P(OMe)_3\}]^+$ (**8**) was investigated theoretically using density functional theory (DFT) and these results are compared with experimental studies of the reactions of $[(\eta^5\text{-}C_5H_5)Fe(CO)_2\{P(OR)_3\}]BF_4$ (R = Me (**8a**), Et (**13**)) with $NaBH_4$ and $NaBH_3CN$ in ethanol, acetone, and THF, together with low-temperature spectroscopic (IR and ^1H NMR) studies of the intermediates formed in the reaction of **8a** with $NaBH_4$.

Results and Discussion

DFT Study of Hydride Attack on $[(\eta^5\text{-}C_5H_5)Fe(CO)_2(PR_3)]^+$ (R = H (1), OMe (8)). In this study two reactions were investigated using DFT: (i) hydride attack on $[(\eta^5\text{-}C_5H_5)Fe(CO)_2(PH_3)]^+$ (**1**) where PH_3 acts as a model phosphine and (ii) hydride attack on $[(\eta^5\text{-}C_5H_5)Fe(CO)_2\{P(OMe)_3\}]^+$ (**8**), where the phosphine ligand is replaced by the phosphite ligand in light of criticisms regarding the use of model ligands such as PH_3.[16−19] In recent years DFT has been shown to be a powerful tool in the study of reaction mechanisms involving transition metal complexes, providing reliable energies and structures which correspond to experimental observations for a wide variety of metal-containing moieties.[20]

The theoretical study of the reactions of **1** and **8** with hydride involved the location of 14 stationary points on both potential energy surfaces. The possible initial attack sites of the hydride anion considered here are shown in Scheme 1. The starter cations **1** and **8** may undergo hydride attack at the phosphorus atom, as proposed by Nakazawa and co-workers,[21] to form the metallophosphorane intermediates $(\eta^5\text{-}C_5H_5)Fe(CO)_2(PH_4)$ (**2**) and $(\eta^5\text{-}C_5H_5)Fe(CO)_2\{P(OMe)_3H\}$ (**9**). Attack can occur at the metal to give the ring-slipped intermediate $(\eta^3\text{-}C_5H_5)Fe(CO)_2(H)(PH_3)$ (**3**) (the analogous phosphite species $(\eta^3\text{-}C_5H_5)Fe(CO)_2(H)\{P(OMe)_3\}$ was not located in this study). The formyl intermediates $(\eta^5\text{-}C_5H_5)Fe(CHO)(CO)(PH_3)$ (**4**) and $(\eta^5\text{-}C_5H_5)Fe(CHO)(CO)\{P(OMe)_3\}$ (**11**) result from attack at the carbon atom of one of the carbonyl groups, and attack at the coordinated C_5H_5 ring leads to the formation of the ring adducts $(\eta^4\text{-}C_5H_6)Fe(CO)_2(PH_3)$ (**7**) and $(\eta^4\text{-}C_5H_6)Fe(CO)_2\{P(OMe)_3\}$ (**12**).

Once these intermediates are formed, they may react further, and often different intermediates will rearrange to the same products. Nakazawa and co-workers[21] proposed that the metallophosphorane intermediates **2** and **9** underwent a "ligand coupling" reaction[22] to give the hydride $(\eta^5\text{-}C_5H_5)Fe(CO)_2(H)$ (**5**) and free ligand as shown by path i in Scheme 2. However, it is well-known[23] that **5** reacts with a wide variety of phosphine and phosphite ligands to give "monocarbonyl hydrides" such as $(\eta^5\text{-}C_5H_5)Fe(CO)(H)(PH_3)$ (**6**) and $(\eta^5\text{-}C_5H_5)Fe(CO)(H)\{P(OMe)_3\}$ (**11**), as shown by path ii in Scheme 2. Indeed, the in situ reaction of **5** and phosphorus-containing ligands is a useful synthetic route to such monocarbonyl hydrides; therefore, it is expected that the sole hydridic products resulting from the rearrangement of **2** and **9** would be **6** and **11**, respectively.

Scheme 1. Possible Initial Attack Sites of the Hydride Anion H^- on the Cations $[(\eta^5\text{-}C_5H_5)Fe(CO)_2PX_3]^+$(X = H (1), OMe (8)) Considered in This Study

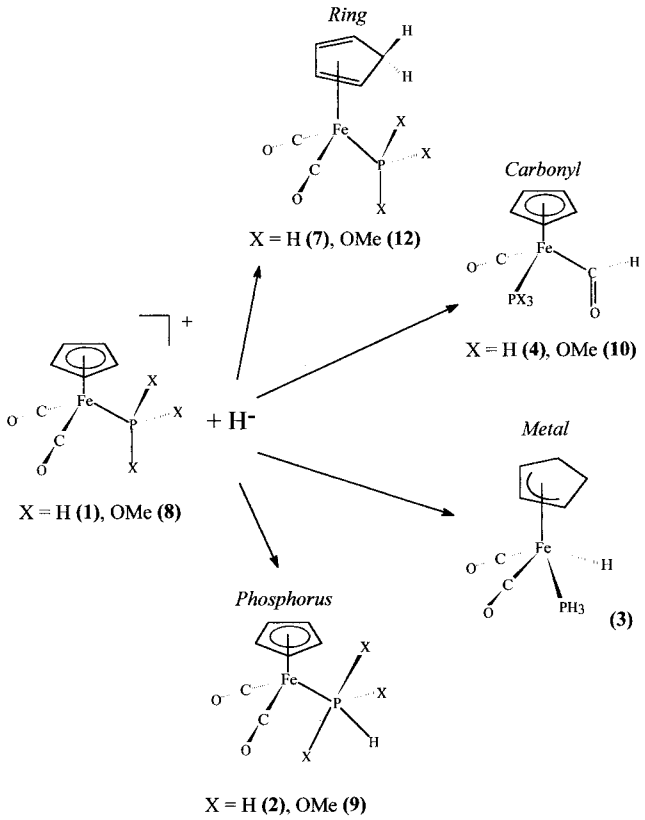

The ring-slipped species **3** may rearrange to give four possible products as shown in Scheme 2 (dashed lines). Migration of the hydrogen atom directly bonded to the metal gives the ring adduct **7** (path a in Scheme 2). In this case the hydrogen atom derived from the reducing agent (such as $NaBH_4$ or $NaBH_3CN$) would be in the *endo* position, whereas in the case of direct hydride attack at the C_5H_5 ring (Scheme 1) the hydrogen atom derived from the reducing agent would be in the *exo* position. This difference in the stereochemistry of the ring adducts has been exploited to determine the mode of reaction.[24] Migratory CO insertion leads to the formyl species **4** (path b in Scheme 2), whereas ligand loss from **3** can lead to the hydride **5** (and PH_3) (path c in Scheme 2) or to the hydride **6** (path d in Scheme 2).

The formyl intermediates, resulting from the direct attack of the hydride at the carbon atom of a carbonyl group (or from the rearrangement of **3** as discussed above) can rearrange in a number of ways, as shown in Scheme 2. Hydride migration leads to the ring adducts **7** and **12** (path iii in Scheme 2). Once again, the

(16) Lin, Z.; Hall, H. B. *J. Am. Chem. Soc.* **1992**, *114*, 2938.
(17) Matsubra, T.; Maseras, F.; Koga, N.; Morokuma, K. *J. Phys. Chem.* **1996**, *100*, 2573.
(18) Jacobsen, H.; Berke, H. *Chem. Eur. J.* **1997**, *3*, 881.
(19) Clot, E.; Eisenstein, O. *J. Phys. Chem. A* **1998**, *102*, 3592.
(20) McCullough, E. A., Jr.; Aprà, E.; Nichols, J. *J. Phys. Chem. A* **1997**, *101*, 2502. Glukhovtsev, M. N.; Bach, R. D.; Nagel, C. J. *J. Phys. Chem. A* **1997**, *101*, 316. Musaev, D. G.; Morokuma, K. *J. Phys. Chem.* **1996**, *100*, 6509. Heinmann, C.; Hertwig, R. H.; Wesendrup, R.; Koch, W.; Schwarz, H. *J. Am. Chem. Soc.* **1995**, *117*, 495. Berces, A.; Ziegler, T.; Fan, L. *J. Phys. Chem.* **1994**, *98*, 1584. Lyne, P. D.; Mingos, D. M. P.; Ziegler, T.; Downs, A. J. *Inorg. Chem.* **1993**, *32*, 4785.
(21) Nakazawa, H.; Kubo, K.; Kai, C.; Miyoshi, K. *J. Organomet. Chem.* **1992**, *439*, C42.
(22) Oae, S.; Uchida, Y. *Acc. Chem. Res.* **1991**, *24*, 202.
(23) Klack, P.; Poilblanc, R. *C. R. Acad. Sci., Ser. C* **1972**, *274*, 66.
(24) Davies, S. G.; Moon, S. D.; Simpson, S. J.; Thomas, S. E. *J. Chem. Soc., Dalton Trans.* **1983**, 1805.

Scheme 2 . Possible Rearrangement and Ligand Loss Reactions of the Initial Attack Products Resulting from the Reaction of H^- with $[(\eta^5\text{-}C_5H_5)Fe(CO)_2PX_3]^+$ (X = H (1), OMe (8))

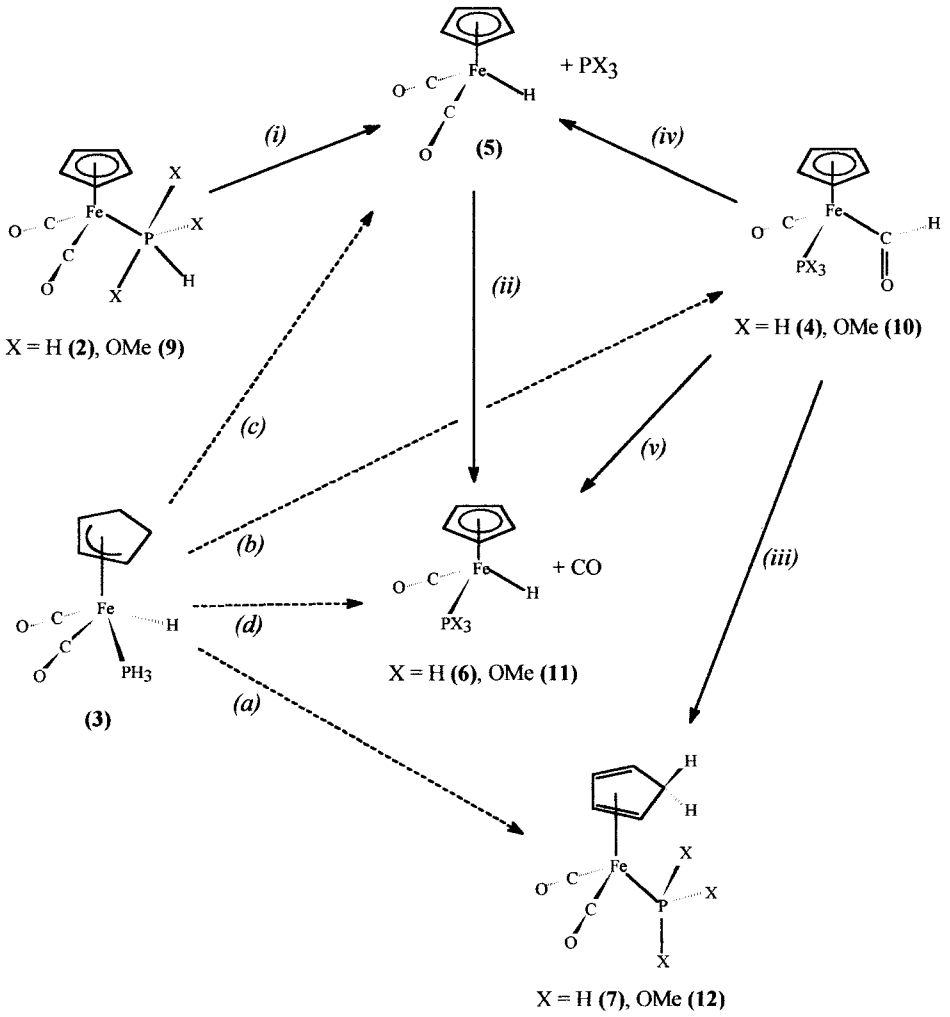

hydrogen atom derived from the reducing agent would be in the *endo* position. The fission of the Fe−P bond in **4** or **10** (with subsequent rearrangement) would lead to **5** and free PX_3 (path iv in Scheme 2), whereas cleavage of the Fe−C(O) bond (and rearrangement) leads to the monocarbonyl hydrides **6** and **11** and free CO (path v in Scheme 2). Again, **5** is expected to react with the free PX_3 ligand to form either **6** or **11** (path ii in Scheme 2), so that the monocarbonyl hydrides would be the sole hydridic products observed from the decomposition of **4** and **10**, respectively.

Finally the ring adducts **7** and **12**, formed by direct attack at the ring (Scheme 1), by rearrangement of **3** (path a in Scheme 2), or via the formyl intermediates (path iii in Scheme 2) are, on the basis of experimental evidence, assumed to be stable species and do not react any further under the conditions considered here. It is interesting to note the contrast with *electrophilic* attack of H^+ on the molybdenum complex $(\eta^6\text{-}C_6H_6)Mo(TRIPOD)$[25] (TRIPOD = 1,1,1-tris((diphenylphosphino)-methyl)ethane), where the ring adduct $[(exo\text{-}\eta^5\text{-}C_6H_7)Mo(TRIPOD)]^+$ is initially formed, but *endo* proton transfer follows to the metal, giving the hydride $[(\eta^6\text{-}C_6H_6)Mo(TRIPOD)(H)]^+$.

(25) Kowalski, A. S.; Ashby, M. T. *J. Am. Chem. Soc.* **1995**, *117*, 12639.

Energy Ordering and Reactivity. (i) Hydride Attack at $[(\eta^5\text{-}C_5H_5)Fe(CO)_2(PH_3)]^+$. On the basis of the reactions presented in Schemes 1 and 2, the study of hydride attack on **1** involved the location of seven minima:

$[(\eta^5\text{-}C_5H_5)Fe(CO)_2(PH_3)]^+$ (**1**)

$(\eta^5\text{-}C_5H_5)Fe(CO)_2(PH_4)$ (**2**)

$(\eta^3\text{-}C_5H_5)Fe(CO)_2(H)(PH_3)$ (**3**)

$(\eta^5\text{-}C_5H_5)Fe(CHO)(CO)(PH_3)$ (**4**)

$(\eta^5\text{-}C_5H_5)Fe(CO)_2(H)$ (**5**)

$(\eta^5\text{-}C_5H_5)Fe(CO)(H)(PH_3)$ (**6**)

$(\eta^4\text{-}C_5H_6)Fe(CO)_2(PH_3)$ (**7**)

In addition, the two transition states **TS1** and **TS2** were located for the intramolecular rearrangement of the formyl species **4** to **5** (**TS1**) and to **6** (**TS2**).

The optimized structures of the minima **1**−**7**, available in the Supporting Information, show the expected trends for these species and correlate well with previous

Table 1. Total and Relative Energies of the Phosphine Complexes 1−7, TS1, and TS2 Obtained at the B3LYP/HUZ1 Level[a]

species[b]	total energy	rel energy[c]
$[(\eta^5\text{-}C_5H_5)Fe(CO)_2(PH_3)]^+ + H^-$ (**1** + H^-)	−2 026.934 740 7	206.70
$(\eta^5\text{-}C_5H_5)Fe(CO)_2(PH_4)$ (**2**)	−2 027.202 502 0	38.70
$(\eta^3\text{-}C_5H_5)Fe(CO)_2(H)(PH_3)$ (**3**)	−2 027.216 101 5	30.16
$(\eta^5\text{-}C_5H_5)Fe(CHO)(CO)(PH_3)$ (**4**)	−2 027.233 738 0	19.00
$(\eta^5\text{-}C_5H_5)Fe(CO)_2(H) + PH_3$ (**5** + PH_3)	−2 027.245 575 0	11.50
$(\eta^4\text{-}C_5H_6)Fe(CO)_2(PH_3)$ (**7**)	−2 027.256 368 0	4.87
$(\eta^5\text{-}C_5H_5)Fe(CO)(H)(PH_3)$ + CO (**6** + CO)	−2 027.264 168 0	0.00
transition state leading to PH_3 loss (**TS1**)	−2 027.191 677 1	45.49, *26.39*[d]
transition state leading to CO loss (**TS2**)	−2 027.186 430 0	48.78, *29.68*[d]

[a] Total energies are given in hartrees and relative energies in kcal mol^{-1}. The relative energies of TS1 and TS2 are also given relative to the formyl complex **4**. [b] The total energies of the hydride, PH_3, and CO ligands are included to allow a comparison of the total energies. [c] These energies are given relative to $(\eta^5\text{-}C_5H_5)Fe(H)(CO)(PH_3)$ **(6)** + CO at the B3LYP/HUZ1 level of theory. [d] The values in italics are calculated relative to the formyl complex $(\eta^5\text{-}C_5H_5)Fe(CHO)(CO)(PH_3)$ **(4)** at the B3LYP/HUZ1 level of theory.

theoretical studies and experimental data, where available. Vibrational frequency analysis was carried out on each of the species **1**−**7**, and all of the structures, apart from **6**, are true minima with no negative frequencies. The scaling factors required to correct the calculated frequencies (of the CO symmetric and antisymmetric stretches) so as to match the experimental values were very close to the value (0.9613) recommended by Wong[26] for this functional. The negative frequency in **6**, at −77 cm^{-1}, corresponds to a rotation of the PH_3 ligand about the Fe−P bond. Since the barrier to rotation about this bond was calculated to be only 0.10 kcal mol^{-1}, the exact location of the rotational minimum was not pursued. The structures obtained for the transition states **TS1** and **TS2**, also given in the Supporting Information, are similar. They both exhibit the "two legged piano stool" configuration commonly observed in 16-electron iron-containing species,[27] and the formyl group is essentially intact in both structures. However, vibrational frequency analysis of **TS1** reveals a significant frequency at −476.0 cm^{-1}, whereas the negative frequency in **TS2** is very low at −29.2 cm^{-1}.

The total and relative energies of **1**−**7** and of **TS1** and **TS2** are given in Table 1, including, where appropriate, the energies of the hydride, CO, and PH_3 ligands. These were calculated using the same basis set as for the complexes, namely 6-31G(d). As an anion basis function was not used for the hydride, the energy of **1** + H^-, compared to that of the neutral species, is somewhat overestimated. However, since the relative energy of **1** + H^- is large (207−168 kcal mol^{-1}) and it is the energy differences between the neutral species that are of most interest, calculations with an anion basis function were not considered.

A number of interesting points emerge from the relative energies presented in Table 1. Consider the initial point of attack of the hydride upon **1**. In this study four possibilities were proposed (Scheme 1), and the energy ordering of these four species is

7 < **4** < **3** < **2**

Thus, attack on the ring leading to the ring adduct **7** is the most energetically favorable pathway. However, it is expected that the energy barrier leading to the formation of **7** is relatively large, because of the repulsion between the π electrons of the cyclopentadienyl ring and the incoming nucleophile, as postulated in the reaction of $[(\eta^5\text{-}C_5H_5)Fe(CO)_3]^+$ and H^-.[15] Thus, the energy barriers leading to the formation of **2**−**4** are expected to be lower than that leading to the formation of the ring adduct **7**. Therefore, while **7** is clearly thermodynamically more stable than **4**, the latter may have a smaller barrier leading to it and formation of both **4** and **7** may take place. A similar situation occurs in the study of the hydride reduction of the cation $[(\eta^6\text{-}C_6H_6)Mn(CO)_3]^+$,[28] where it was found that the formyl species $(\eta^6\text{-}C_6H_6)Mn(CHO)(CO)_2$ lies 50.5 kcal mol^{-1} higher in energy than the ring adduct $(\eta^5\text{-}C_6H_7)Mn(CO)_3$, but both are observed experimentally at room temperature.

The species **2** and **3** are less stable than both the ring adduct **7** and the formyl complex **4**, and since there is no evidence that the energy barriers leading to the formation of **2** and **3** would be any lower than that leading to the formation of **4**, both **3** and, in particular, **2** (which lies 19.7 kcal mol^{-1} above **4** and 33.83 kcal mol^{-1} above **7**) are predicted to be too high in energy to be intermediates in this reaction. Thus, the metallophosphorane intermediate **2**, although located as a minimum on this potential energy surface, is not expected to be formed in the hydride reduction of species such as $[(\eta^5\text{-}C_5H_5)Fe(CO)_2(\text{phosphine})]^+$, whereas the formyl species **4** and the ring adduct **7** are predicted to be the initial products resulting from attack by the hydride.

Once the formyl species **4** is formed, it can react further in a number of ways (Scheme 2). One possibility is an intramolecular rearrangement leading to the ring adduct **7**, (path iii in Scheme 2), as occurs in the hydride reduction of $[(\eta^6\text{-}C_6H_6)Mn(CO)_3]^+$,[10] and as the ring adduct **7** here is more stable than the formyl **4**, such a pathway is energetically favorable. The formyl species **4** can also undergo loss of PH_3 to give the dicarbonyl hydride **5** (path iv in Scheme 2) or loss of CO to give the monocarbonyl hydride **6** (path v in Scheme 2). Since **6** is relatively more stable than **5**, by 11.50 kcal mol^{-1}, it would be expected that **6** + CO would be formed in preference to **5** + PH_3.

However, if the energy barrier from **4** to **5** + PH_3 was similar to, or lower than, that from **4** to **6** + CO, then some **5** could be formed, which would react with free PH_3 to give **6** + CO. In other words, two paths for the formation of **6** are possible—it may be formed either directly from **4** (path v in Scheme 2) or via **5** and PH_3 (path iv and then ii in Scheme 2). To investigate which path is favored, the two transition states **TS1** and **TS2** have been located. **TS1** is the transition state found for the decomposition of **4** leading to **5** and PH_3, whereas

(26) Wong, M. W. *Chem. Phys. Lett.* **1996**, *256*, 391.
(27) Ward, T. R.; Schafer, O.; Daul, C.; Hofmann, P. *Organometallics* **1997**, *16*, 3207.
(28) Conlon, P. C. Ph.D. Thesis, National University of Ireland, 1994, p 69.

TS2 is the transition state for the decomposition of **4** leading to **6** and CO. **TS1** and **TS2** lie 26.39 and 29.68 kcal mol^{-1}, respectively, above **4** at the B3LYP/HUZ1 level; therefore, the total energies of **TS1** and **TS2** differ by approximately 3 kcal mol^{-1}. While the values relative to **4** need to be treated with caution, the energy difference between **TS1** and **TS2** should remain close, which implies that the energy barriers leading to the formation of **5** and **6** are very close. Thus, it is predicted that both pathways to **6** (paths iv and v in Scheme 2) are possible but that since **5** reacts with free PH_3 (path ii in Scheme 2), **6** would be the sole hydridic product resulting from the reduction of **1**.

The conclusions presented above agree with experimental evidence for the reduction of phosphine-containing species such as $[(\eta^5\text{-}C_5H_5)Fe(CO)_2(PPh_3)]^+$ [4,24] and $[(\eta^5\text{-}C_5H_5)Fe(CO)_2(PMe_3)]^+$,[29] albeit with some discrepancies. For the reduction of $[(\eta^5\text{-}C_5H_5)Fe(CO)_2(PPh_3)]^+$ with $LiAlH_4$[4,24] both the ring adduct $(\eta^4\text{-}C_5H_6)Fe(CO)_2(PPh_3)$ and the monocarbonyl hydride $(\eta^5\text{-}C_5H_5)Fe(CO)(H)(PPh_3)$ are formed, but not the expected formyl complex $(\eta^5\text{-}C_5H_5)Fe(CHO)(CO)(PPh_3)$. Initial formation of $(\eta^5\text{-}C_5H_5)Fe(CO)_2H + PPh_3$, followed by formation of $(\eta^5\text{-}C_5H_5)Fe(H)(CO)(PPh_3) + CO$, was not considered, although such a pathway is feasible.[23]

As noted above, the stereochemistry of the ring adduct $(\eta^4\text{-}C_5H_6)Fe(CO)_2(PPh_3)$ is a crucial piece of evidence in understanding the reaction path. Reduction of $[(\eta^5\text{-}C_5H_5)Fe(CO)_2(PPh_3)]^+$ with a range of reducing agents gives only the *exo* isomer, confirming that "stereospecific *exo* addition had occurred"[24] and that the ring adduct is formed in this case by direct attack at the ring (Scheme 1) and not by rearrangement of **4**, as proposed in path iii of Scheme 2. The reason for the exclusive formation of the *exo* isomer may lie with the energy barrier for the rearrangement of **4** to **7**. If this barrier were high, or more specifically higher relative to **TS1** and **TS2**, then **4** would undergo ligand loss in preference to rearrangement. Thus, the only pathway leading to **7** would be via direct ring attack, giving exclusively the *exo* $(\eta^4\text{-}C_5H_6)Fe(CO)_2(PPh_3)$ isomer.

In the reduction[29] of $[(\eta^5\text{-}C_5H_5)Fe(CO)_2(PMe_3)]^+$ by $LiAlH_4$, the sole product is the methyl complex $(\eta^5\text{-}C_5H_5)Fe(CH_3)(CO)(PMe_3)$, formed from the observed formyl complex $(\eta^5\text{-}C_5H_5)Fe(CHO)(CO)(PMe_3)$ (δ(C*H*O) 15.4 ppm, d; $J_{P-H} = 5$ Hz). The ring adduct $(\eta^4\text{-}C_5H_6)Fe(CO)_2(PMe_3)$ was not observed. In this case the strongly electron donating PMe_3 ligand not only directs attack exclusively to the carbonyl ligand but also stabilizes the formyl intermediate thus formed with respect to decomposition to the possible hydridic products, thereby allowing complete reduction to the methyl complex. Although the formation of the methyl complex was not explicitly considered in the present study, the ring adduct **7** was predicted to be more stable than the formyl species **4**. Thus, while the PH_3 ligand used here successfully models reactions involving PPh_3, it is not suitable for reactions involving strongly electron donating ligands such as PMe_3, a result similar to that obtained in previous theoretical studies using PH_3.[16−19]

(ii) Hydride Attack at $[(\eta^5\text{-}C_5H_5)Fe(CO)_2\{P(OMe)_3\}]^+$. Five minima were located for this system:

(29) Brown, S. L.; Davies, S. G.; Simpson, S. J.; Thomas, S. E. *Appl. Catal.* **1986**, *25*, 84.

Table 2. Total and Relative Energies of the Phosphite Complexes 8−12 and 5 Obtained at the B3LYP/HUZ1 Level[a]

species[b]	total energy	rel energy[c]
$[(\eta^5\text{-}C_5H_5)Fe(CO)_2\{P(OMe)_3\}]^+ + H^-$ (**8** + H^-)	−2 370.718 204 9	204.74
$(\eta^5\text{-}C_5H_5)Fe(CO)_2\{P(OMe)_3H\}$ (**9**)	−2 371.001 463 3	27.00
$(\eta^5\text{-}C_5H_5)Fe(CHO)(CO)\{P(OMe)_3\}$ (**10**)	−2 371.024 181 9	12.74
$(\eta^5\text{-}C_5H_5)Fe(CO)_2(H) + P(OMe)_3$ (**5** + $P(OMe)_3$)	−2 371.026 846 6	11.05
$(\eta^5\text{-}C_5H_5)Fe(CO)(H)\{P(OMe)_3\} + CO$ (**11** + CO)	−2 371.032 737 9	7.37
$(\eta^4\text{-}C_5H_6)Fe(CO)_2\{P(OMe)_3\}$ (**12**)	−2 371.044 478 9	0.00

[a] Total energies are given in hartrees and relative energies in kcal mol^{-1}. [b] The total energies of the hydride, $P(OMe)_3$, and CO ligands are included to allow a comparison of the total energies. [c] These energies are given relative to $(\eta^4\text{-}C_5H_6)Fe(CO)_2\{P(OMe)_3\}$ **(12)** at the B3LYP/HUZ1 level of theory.

$[(\eta^5\text{-}C_5H_5)Fe(CO)_2\{P(OMe)_3\}]^+$ (**8**)

$(\eta^5\text{-}C_5H_5)Fe(CO)_2\{P(OMe)_3H\}$ (**9**)

$(\eta^5\text{-}C_5H_5)Fe(CHO)(CO)\{P(OMe)_3\}$ (**10**)

$(\eta^5\text{-}C_5H_5)Fe(CO)(H)\{P(OMe)_3\}$ (**11**)

$(\eta^4\text{−}C_5H_6)Fe(CO)_2\{P(OMe)_3\}$(**12**)

Note that **5** is a common intermediate in the reactions of both the phosphine and phosphite species and has already been located. However, to calculate the relative energies, the structure of the ligand $P(OMe)_3$ was optimized at the B3LYP/HUZ1 level. Numerous attempts to locate the ring-slipped species $(\eta^3\text{-}C_5H_5)Fe(CO)_2P(OMe)_3H$ for this system, analogous to **3**, were unsuccessful. No searches were undertaken for any transition structures, and no vibrational frequency analysis was carried out for any of the species **8**−**12**. In the latter stages of the optimizations of the species **8**−**12** the geometry of the methyl groups in the $P(OMe)_3$ ligand was fixed, as were the O−C distances within this ligand.

Once again the optimized structures of the species **8**−**12**, provided in the Supporting Information, exhibit the trends expected for complexes of this type. So, for example, the Fe−P bond lengths in **8**−**12** are always lower than in the analogous phosphine complexes because $P(OMe)_3$ is a poorer σ donor but a better π acceptor than PH_3. Apart from this change, however, the structural changes induced by the substitution of $P(OMe)_3$ for PH_3 are slight so that from a structural point of view PH_3 is an adequate model for $P(OMe)_3$.

The total and relative energies of the phosphite species **8**−**12**, and those of the common intermediate **5** + $P(OMe)_3$, are given in Table 2. Again it is of interest to consider the initial point of attack of the hydride on $[(\eta^5\text{-}C_5H_5)Fe(CO)_2(POMe_3)]^+$ (**8**). For this system three possibilities can be considered (Scheme 1) and the energy ordering of these three species is

12 < **10** < **9**

Therefore, as before, the formation of the ring adduct is the most thermodynamically favorable pathway; the energy difference between the ring adduct **12** and the formyl species **10** is 12.74 kcal mol^{-1}, slightly less than

Table 3. Products Obtained upon the Reduction of the Species 8a and 13 with $NaBH_4$ and $NaBH_3CN$ at Room Temperature in the Solvent Indicated

substrate	solvent		
	EtOH	acetone	THF
$[(\eta^5\text{-}C_5H_5)Fe(CO)_2\{P(OMe)_3\}]BF_4$ (**8a**)	$(\eta^5\text{-}C_5H_5)Fe(CO)(H)\{P(OMe)_3\}$ (**9**) and $(\eta^4\text{-}C_5H_6)Fe(CO)_2\{P(OMe)_3\}$ (**12**) (minor product)	**9** and **12**	**12**
$[(\eta^5\text{-}C_5H_5)Fe(CO)_2\{P(OEt)_3\}]BF_4$ (**13**)	$(\eta^5\text{-}C_5H_5)Fe(CO)H\{P(OEt)_3\}$ (**14**) and $(\eta^4\text{-}C_5H_6)Fe(CO)_2\{P(OEt)_3\}$ (**15**) (minor product)	**14** and **15**	**15**

the same value for the phosphine system. As before, the energy barrier leading to the formation of **12** is probably larger than that leading to the formation of **10**, so that both **12** and **10** would be expected to be formed. It is noteworthy that the relative energy of the metallophosphorane adduct **9** is lower than that in the phosphine system; **9** lies 27.0 kcal mol^{-1} above the ring adduct **12**. For the analogous phosphine species this energy difference was 33.8 kcal mol^{-1}, so that the effect of the replacement of the phosphine by the phosphite ligand is to stabilize the metallophosphorane adduct relative to the other species that may be formed.

As in the previous system, once the formyl **10** is formed, it can react further (Scheme 2). As before, an intramolecular rearrangement of **10** to yield the ring adduct is feasible (path iii in Scheme 2), because **12** is predicted to be more stable than **10**. Also possible is the loss of $P(OMe)_3$ from **10** to give **5** (path iv in Scheme 2), or the loss of CO to give **11** (path v in Scheme 2). The monocarbonyl hydride species **11** + CO is again relatively more stable than the dicarbonyl hydride species **5** + $P(OMe)_3$, but the energy difference between them is now only 3.68 kcal mol^{-1}. This small energy difference, coupled with the fact that it is expected that the energy barriers from **10** to the two hydrides are similar, as in the phosphine system, implies that both species could result from the decomposition of **10**. Since the relative energy of **5** and $P(OMe)_3$ is above that of **11** and CO, it is clear that if **5** were formed it would combine with any free ligand to give **11** (path ii in Scheme 2), which would be the sole hydridic product observed.

These conclusions for the phosphite system are now compared with the experimental evidence for the reduction of $[(\eta^5\text{-}C_5H_5)Fe(CO)_2P(OR)_3)]BF_4$ (R = Me (**8a**), Et (**13**)).

B. Experimental Studies of the Reduction of $[(\eta^5\text{-}C_5H_5)Fe(CO)_2(P(OR)_3]^+$ (R = Me (8a), Et (13)). (i) Reduction Reactions of $[(\eta^5\text{-}C_5H_5)Fe(CO)_2\{P(OR)_3\}]BF_4$ (R = Me, Et) at Room Temperature. The reduction of **8a** and **13** was studied at room temperature in three different solvents (THF, acetone, and ethanol) using the two different hydride sources $NaBH_4$ and $NaBH_3CN$. These reactions were studied to investigate the effect of the solvent and the hydride source on the products isolated. Low-temperature spectroscopic (IR and ^1H NMR) investigations were then carried out on the reduction of **8a** in acetone using $NaBH_4$.

The products obtained upon the reduction of the cations **8a** and **13** at room temperature are summarized in Table 3. It is clear that the reduction of these species exhibits a marked solvent dependence but is independent of the hydride source used; however, the reaction times using $NaBH_3CN$ were appreciably longer. In ethanol (Table 3), the ring adducts **12** and **15** are formed, as evidenced by the IR spectrum of the reaction mixture, but only in very small amounts compared to the hydrides **11** and **14**, whereas both the hydrides and the ring adducts are formed to an appreciable extent in acetone.

As noted above, the stereochemistry of the ring adducts **12** and **15** is an important piece of evidence in understanding these reactions. Direct attack from the less sterically hindered *exo* face of the cyclopentadienyl ring leads to the formation of the *exo* isomer, whereas rearrangement of an intermediate such as the formyl species **10** (path iii in Scheme 2), would lead to the *endo* isomer. In the case of hydride attack, the *exo* and *endo* isomers are indistinguishable, but the *endo* and *exo* protons of the ring adducts can be assigned in the ^1H NMR spectrum by exploiting the long-range coupling with the phosphorus atom of the phosphite ligand.[24] H_{exo} appears as a triplet, because it is in the correct geometric arrangement to couple with the phosphorus atom, whereas H_{endo} appears as a doublet, upfield from H_{exo}.

Using the fact that the *exo* and *endo* protons are easily identified, the stereochemistry of the addition was investigated by reducing **8a** with $NaBD_4$ in both acetone and THF. In both cases the *exo* isomer (*exo*-η^4-C_5H_5D)-$Fe(CO)_2\{P(OMe)_3\}$ was formed. The ^1H NMR of this species shows that the triplet assigned to H_{exo} above had disappeared, whereas H_{endo} appears as a broad singlet, as the proton−deuteron coupling constant is typically 10−15% of the corresponding proton−proton value and cannot be resolved here. This implies that the initial site of attack is solvent dependent. Direct ring attack from the *exo* side of the ring occurs exclusively in THF and attack at one of the carbonyl groups to form a formyl intermediate, which then loses a CO ligand to give the hydride, is predominant in ethanol, whereas both occur to an appreciable extent in acetone. Eyman and coworkers,[10] in their studies of the hydride reduction of $[(\eta^6\text{-}C_6H_6)Mn(CO)_3]^+$ and $[(\eta^6\text{-}C_6(CH_3)_6)Mn(CO)_3]^+$, observed a similar solvent dependence. They observed that attack at one of the carbonyl ligands was predominant in methanol, forming a formyl intermediate (which incidentally rearranged to a ring adduct). They proposed an interesting explanation for this which may account for the predominant formation, in this study, of the monocarbonyl hydrides **11** and **14** in ethanol. The cations **8a** and **13** are only sparingly soluble in this solvent at room temperature. Any undissolved cation at the solvent−crystal interface is oriented so that the more hydrophilic part of the molecule, the carbonyl and phosphite ligands, points toward the solvent. Thus, attack at the carbonyl ligands, assuming no metallophosphorane intermediate is formed, is favored in ethanol. Since the cations are freely soluble in acetone, attack at both the carbonyl and cyclopentadienyl ligands occurs in this solvent. In dry THF, as for those manga-

nese cations studied by Eyman and co-workers[10] and for those cations studied here, attack occurs exclusively at the *exo* side of the coordinated ring, leading to the sole formation of the *exo* isomer.

(ii) Low-Temperature Studies of the Reaction of $[(\eta^5\text{-}C_5H_5)Fe(CO)_2\{P(OMe)_3\}]BF_4$ with $NaBH_4$ in Acetone. The mechanism of the hydride reduction of **8a** was investigated by studying the reaction of this cation with $NaBH_4$ in acetone at low temperatures. Acetone was chosen because **8a** is freely soluble, even down to the freezing point −94 °C, in this solvent.

Initial investigations were carried out using a special low-temperature IR cell. The reaction mixture was held at −80 °C, and an aliquot was taken and rapidly transferred to the cell, which was also held at −80 °C. The spectrum taken at this temperature showed a peak at 2013 cm^{-1} and a very broad peak at 1946 cm^{-1} with shoulders at 1977 and 1920 cm^{-1}. The peak at 2013 cm^{-1} was assigned to the hydride **5**, by comparison with previous studies.[30] The shoulders at 1977 and 1920 cm^{-1} are due to the ring adduct **7**, as observed above. The very broad peak centered at 1946 cm^{-1} may be due to overlap of three separate peaks: (i) the other ν(CO) stretch of the hydride **5** which is expected to appear[30] at 1952 cm^{-1}, (ii) the single ν(CO) stretch of the hydride **11**, observed at 1937 cm^{-1} in acetone above, and (iii) speculatively, the *carbonyl* stretch of the remaining carbonyl group in the formyl species **10**. In the vibrational frequency analysis performed on the analogous species **4**, this stretch was predicted to appear at 1973 cm^{-1}, using a scaling factor of 0.9613.[26] Thus, it is plausible that the broad peak observed obscures this stretch. Unfortunately, the characteristic CO stretch of the formyl group itself cannot be observed in acetone.

Given the uncertainty over the presence of a formyl intermediate, the reaction was studied using low-temperature ^1H NMR. A sample of **8a** and $NaBH_4$ were mixed in d_6-acetone at −80 °C and transferred to the probe of the spectrometer, which was also at −80 °C. The temperature was then raised in increments of 5 °C, and spectra were recorded. The spectrum recorded at −80 °C shows, apart from the signals in the 0−6 ppm region, four new signals at δ 14.48, −12.00, −13.53, and −13.86 ppm. The signal at δ 14.48 ppm can be assigned with some confidence to the proton in the −CHO group of the formyl species $(\eta^5\text{-}C_5H_5)Fe(CO)(CHO)P(OMe)_3$ by a comparison of this value with those observed for similar species, including $(\eta^5\text{-}C_5H_5)Fe(CO)(CHO)PMe_3$ (δ 15.40 ppm),[29] $(\eta^5\text{-}C_5Me_5)Fe(CHO)(CO)PPh_3$ (δ 14.26 ppm),[31a] $(\eta^5\text{-}C_5H_5)Fe(CHO)(CO)_2$ (δ 14.15 ppm),[31b] and $(\eta^5\text{-}C_5Me_5)Fe(CHO)(CO)_2$ (δ 13.72 ppm).[31a] Similarly, the signal at δ −12.00 ppm can be assigned to the well-known hydride **5**.[30] The signals at δ −13.53 and −13.86 ppm are in fact a doublet and can be assigned to the hydride **11**, with a J_{P-H} coupling constant of 89.5 Hz, by a comparison with the spectrum of the same compound obtained at room temperature. The observation of **5** implies the loss of $P(OMe)_3$ from the starter cation and hence the presence of free $P(OMe)_3$ in solution. Two doublets can be observed in this spectrum at δ 3.52 and 3.64 ppm. The former, with a J_{P-H} coupling constant of 11.7 Hz, is due to the methyl protons of the phosphite ligand in the species **11**. The latter, with a J_{P-H} coupling constant of 10.3 Hz, can be assigned to the methyl protons of the free $P(OMe)_3$ ligand.

As the temperature is raised, the signal at δ 14.48 ppm gradually diminishes in intensity and at −50 °C has completely disappeared. The signals for the hydrides meanwhile have increased in intensity. This is consistent with the gradual conversion of the formyl species **10** to either **11** and CO or to **5** and free $P(OMe)_3$ as the temperature is raised. The conversion of the formyl species to either of the two hydrides is complete at −50 °C. As the temperature is raised further, the signal at δ −12.00, assigned to the hydride **5**, gradually disappears, and by −25 °C the only signals observed below 0 ppm is the doublet at δ −13.53 and −13.86 due to the monocarbonyl hydride **11**. This is consistent with the reaction of **5** and the free $P(OMe)_3$ to give **11** as observed by Klack and Poilblanc.[23] No further change occurs as the probe is warmed to room temperature.

It should be noted that no signals are observed, at any temperature, that would be consistent with the formation of a metallophosphorane or any ring-slipped species. No experimental data exist for species where both a transition-metal moiety and a hydrogen atom are bound to a pentacordinated phosphorus atom, but numerous organic phosphoranes with P−H bonds are known.[32] The signal for the proton directly bound to the phosphorus atom in such species usually appears in the region δ 5.5−8.5 ppm, and the J_{P-H} coupling constants are very large, 300−600 Hz. This resonance is expected to be shifted downfield in a metallophosphorane with a P−H bond, analogous to the downfield shift observed for the P−H proton for free PPh_2H (δ 5.20 ppm, d; J_{P-H} = 218 Hz) compared to the complex $[(\eta^5\text{-}C_5H_5)Fe(CO)_2\text{-}PPh_2H]^+$ (δ 7.67 ppm, d; J_{P-H} = 413.4 Hz).[21] The only signal observed above δ 6 ppm here was the singlet at δ 14.48 ppm, assigned to the formyl species **10**. Using a similar argument, it is expected that the formation of the ring-slipped species $(\eta^3\text{-}C_5H_5)Fe(H)(CO)_2P(OMe)_3$ would be indicated by the presence of a signal below δ 0 ppm, due to the proton directly bound to the iron atom. Such a signal was observed in a previous study for the species $(\eta^3\text{-}C_9H_7)Fe(CO)_3H$ at δ −8.75 (s) ppm,[33] but in the present study the only signals observed below δ 0 ppm were those unambiguously assigned to the hydrides **5** and **11**. In summary, no evidence was found for the formation of any metallophosphorane or ring-slipped intermediates in the reaction of $NaBH_4$ with **8a**. A proposed reaction scheme, based on the low-temperature IR and ^1H NMR evidence presented here, is shown in Scheme 3.

Finally, it is interesting to note that the experimental evidence shows that the hydrides **5** and **11** are formed to an appreciable extent from the formyl **11**. This suggests that the barrier heights for the reactions **10** → **11** + CO and **10** → **5** + $P(OMe)_3$ are similar. This observation is in agreement with the theoretical predictions, albeit for the phosphine system, that the relative

(30) Shackleton, T. A.; Mackie, S. C.; Fergusson, S. B.; Johnston, L. J.; Baird, M. C. *Organometallics* **1990**, *9*, 2248.
(31) (a) Lapinte, C.; Catheline, D.; Astruc, D. *Organometallics* **1988**, *7*, 1683. (b) Brown, D. A.; Glass, W. K.; Salama, M. M. *J. Organomet. Chem.* **1994**, *474*, 129.
(32) Dillon, K. B. *Chem. Rev.* **1994**, *94*, 1441 and references therein.
(33) Ahmed, H.; Brown, D. A.; Fitzpatrick, N. J.; Glass, W. K. *J. Organomet. Chem.* **1991**, *418*, C14.

Scheme 3 . Proposed Mechanism for the Reaction of $[(\eta^5\text{-}C_5H_5)Fe(CO)_2\{P(OMe)_3\}][BF_4]$ (8a) and $NaBH_4$ in d_6-Acetone at −80 to +20 °C

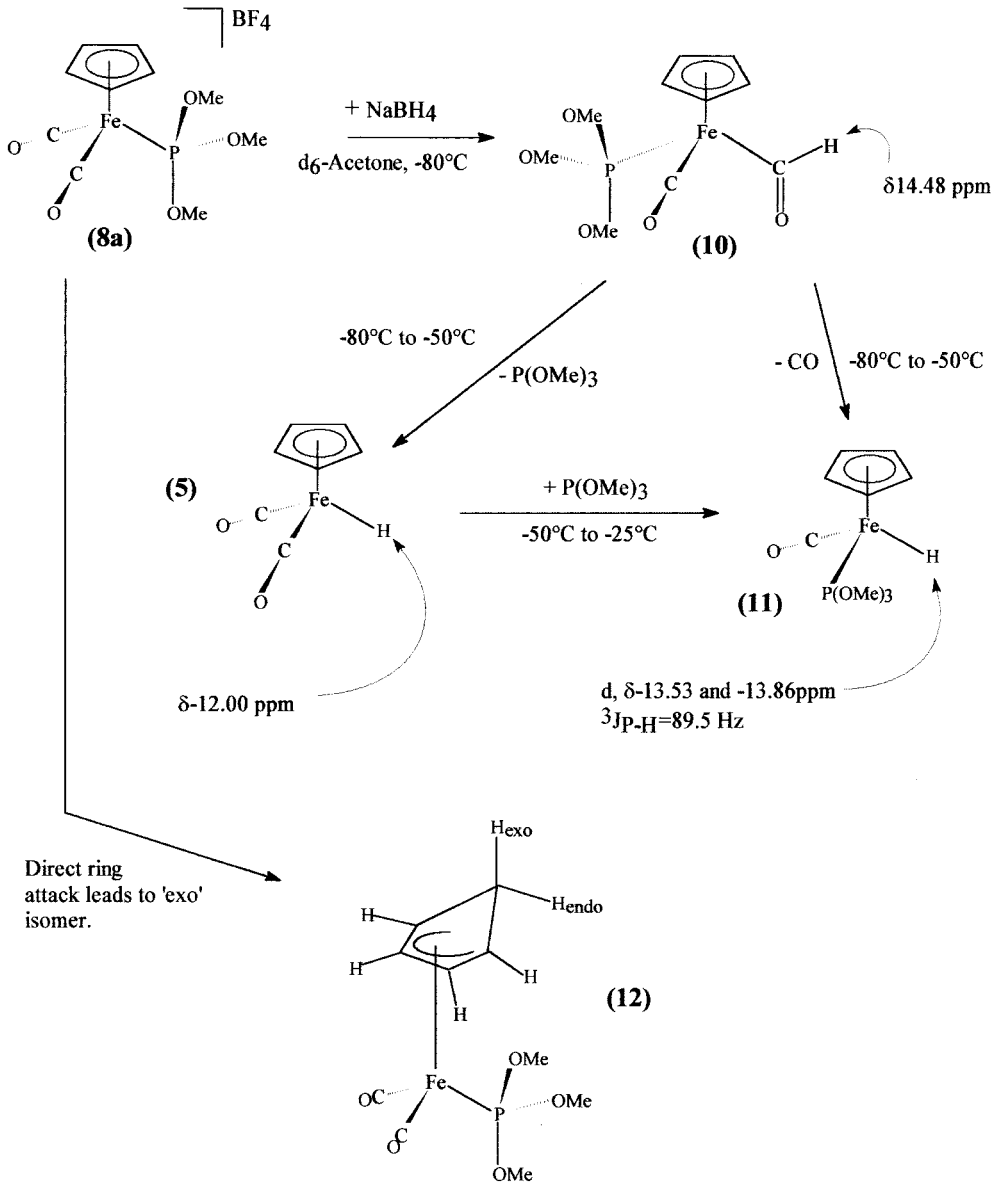

energies of the two transition states located for the rearrangement of the formyl species, **TS1** and **TS2**, are very close in energy.

Conclusion

The hydride reduction of two mononuclear organometallic cations **1** and **8** was studied using DFT. From a comparison of the relative energies of the 14 stationary points located on both potential energy surfaces, it was deduced that the most energetically favorable sites of attack were the coordinated cyclopentadienyl ring, leading to the ring adducts **7** and **12**, and one of the CO ligands, leading to the formyl species **4** and **10**. While the metallophosphorane species **2** and **9** were located, it was predicted that the relative energies of these complexes, compared to the formyl species, were too high and that they would not be formed in the reduction reaction. The ring-slipped species **3** was also located, but once again its relative energy was significantly higher than that of the formyl **4**. The three hydrides **5**, **6**, and **11** were also located, and the relative energies of these species were below those of **4** and **10**; thus, ligand loss from the formyl species **4** and **10** was found to be energetically favorable. It was also predicted that the hydride **5** would react with free phosphine or a phosphite ligand to give **6** or **10**, so that these monocarbonyl hydrides would be the sole hydridic products resulting from the reduction of the starter cations. In addition, the two transition states **TS1** and **TS2** were located for the decomposition of the formyl species **4** to either **5** or **6**. The relative energies of **TS1** and **TS2** were very close, leading to the conclusion that both hydrides may be formed as a result of the decomposition of **1**.

These predictions were found to be borne out by an experimental study of the reduction of the cations **8a** and **13** at room temperature, where, depending on the solvent, the ring adducts **12** and **15** or the monocarbonyl hydrides **10** and **14** were isolated and characterized. To study the reaction further, the reduction of **8a** by $NaBH_4$ in d_6-acetone was studied using low-temperature ^1H NMR. Signals corresponding to the formyl intermediate

10 and the hydrides **5** and **11** were observed at −80 °C. As the temperature was raised, the signal for the formyl **10** diminished, while those of the hydrides increased, consistent with the gradual conversion of **10** to either **5** or **11**, in agreement with the theoretical predictions. As the temperature was raised further, the signal for the hydride **5** diminished, while that of the hydride **11** remained, consistent with the reaction of **5** with free $P(OMe)_3$, as predicted by theory. No signals were observed which would indicate the formation of any metallophosphorane or ring-slipped species.

Finally, a comparison of these studies, concerning nucleophilic attack by hydride, with those of electrophilic attack by protons[34] on the closely related (η^6-arene)$Mo(PR_3)_3$ (R = Ph, Me) and (η^6-C_6H_6)Mo(TRIPOD) (TRIPOD = 1,1,1-tris((diphenylphosphino)methyl)ethane) is instructive. In the latter case, competition between direct attack at the metal and *exo* attack on the arene (benzene) ring occurs, with the latter being promoted by the TRIPOD ligand shielding the e symmetry orbital. In contrast, our results, both theoretical and experimental, give no evidence for initial metal attack leading directly to the metal hydrides or initial ring attack leading directly to the metal hydrides; rather, we find that these species are formed from the corresponding formyls **4** and **10**.

Experimental Section

General Comments. All solvents were freshly dried by standard methods. All reactions were carried out under a nitrogen atmosphere. The phosphites $P(OMe)_3$ and $P(OEt)_3$ and the diphosphine $PPh_2(CH_2)_3PPh_2$ were obtained commercially and used without further purification. The hydrides $NaBH_4$ and $NaBH_3CN$ were also obtained commercially and stored under argon. The complexes [(η^5-C_5H_5)Fe(CO)$_2${P(OR)$_3$}]-BF_4 (R = Me (**8a**), Et (**13**)) were prepared as described previously.[35] Infrared spectra in the carbonyl region were recorded on a Perkin-Elmer 1720 spectrophotometer using a CaF_2 cell. The low-temperature IR spectra were obtained using a Specac P/N 21.500 variable-temperature cell. All NMR spectra, including the low-temperature spectra, were obtained on a JEOL GX270 spectrometer at the NMR Center of the UCD Chemical Services Unit. All microanalyses were carried out by the Microanalytical Laboratory of the Chemistry Department, University College Dublin.

Reduction of 8a using $NaBH_4$ and $NaBH_3CN$. The reduction of **8a** was carried out using two different hydride sources ($NaBH_4$ and $NaBH_3CN$) in three different solvents (EtOH, acetone, and THF). A typical procedure is given.

To 1.0 g (2.58 mmol) of **8a**, dissolved in 40 mL of the solvent, was added an equimolar amount of fresh $NaBH_4$ (0.10 g, 2.58 mmol) or $NaBH_3CN$ (0.16 g, 2.58 mmol). When the reaction was carried out in ethanol, an excess of $NaBH_4$ had to be used, because this reagent decomposes in this solvent. After completion of the reaction, as evidenced by the disappearance of the carbonyl stretching peaks of **8a**, about 1 mL of water was added to the reaction mixture to consume any unreacted hydride reagent. The reduction products were then extracted from the reaction mixture using petroleum ether (40−60 °C), the extracts were dried over $MgSO_4$, and the volume was reduced under vacuum. This solution was then chromatographed on an alumina column using petroleum ether (40−60 °C) as eluant. The procedure for this varied depending on the choice of solvent. For reactions carried out in ethanol, the first 10 mL (approximately) to elute was a mixture of the hydride **11** and the ring adduct **12**. Attempts to separate these products by chromatography a second time were unsuccessful because none of the ring adduct could be isolated. **11** was isolated as an amber liquid by collecting what remained on the column and removing the solvent under reduced pressure. For the reaction in acetone, it proved possible to isolate the ring adduct **12** as a tan liquid by rechromatography of the first 25 mL (approximately) to elute, reducing the volume of the solution under vacuum, cooling in an acetone/dry ice bath, filtering cold, and finally removing all of the solvent. The hydride **11** was also isolated. In THF only **12** is formed**,** the solution of which (after chromatography) was filtered cold and the solvent removed under vacuum.

(η^5-C_5H_5)Fe(CO)(H)P(OMe)$_3$ (**11**): IR (cm^{-1}, acetone) ν(CO) 1937; ^{1}H NMR (δ, d_6-acetone) 4.59 (d, J_{P-H} = 1.0 Hz, 5H, C_5H_5), 3.51 (d, 11.5 Hz, J_{P-H} = 11.5 Hz, 9H, (−OCH_3)$_3$), −13.70 (d, J_{P-H} = 89.5 Hz, 1H, Fe*H*); ^{13}C NMR (δ, d_6-acetone) 195.4 (d, J_{P-C} = 36.6 Hz, Fe*C*O), 88.2 (s, C_5H_5), 55.1 (d, J_{P-C} = 6.5 Hz, (−O*C*H$_3$)$_3$); ^{31}P NMR (δ, d_6-acetone) 204.9 (s, −*P*(OMe)$_3$). Anal. Calcd for $C_9H_{15}FeO_4P$: C, 39.45; H, 5.52; P, 11.83. Found: C, 39.57; H, 5.29; P, 10.84.

(η^4-C_5H_6)Fe(CO)$_2$P(OMe)$_3$ (**12**): IR (cm^{-1}, acetone) ν(CO) 1978, 1917; ^{1}H NMR (δ, d_6-acetone) 5.25 (s, 2H, H_2, H_3 (inner)), 3.26 (d, 11.7 Hz, J_{P-H} = 11.5 Hz, 9H, (−OCH_3)$_3$), 2.78 (d, J_{H-H} = 11.0 Hz, 1H, H_{endo}), 2.62 (s, 2H, H_1, H_4 (outer)) 2.34 (t, J_{H-H} = 11.0 Hz, J_{P-H} = 10.1 Hz, 1H, H_{exo}); ^{13}C NMR (δ, d_6-acetone) 203.5 (d, J_{P-C} = 42.0 Hz, Fe*C*O), 90.4 (s, C_2, C_3), 63.1 (s, C_1, C_4), 50.9 (d, J_{P-C} = 7.5 Hz, (−O*C*H$_3$)$_3$), 46.4 (s, C_5); ^{31}P NMR (δ, d_6-acetone) 187.8 (s, −*P*(OMe)$_3$). Anal. Calcd for $C_{10}H_{15}FeO_5P$: C, 39.79; H, 5.01; P, 10.26. Found: C, 40.20; H, 5.06; P, 9.67.

Reaction of 8a with $NaBD_4$. This reaction was carried out in acetone in exactly the same manner as described above and the product characterized by ^{1}H NMR.

(η^4-C_5H_5D)Fe(CO)$_2$P(OMe)$_3$ (**12a**): ^{1}H NMR (δ, d_6-C_6D_6) 5.25 (s, 2H, H_2, H_3 (inner)), 3.26 (d, 11.7 Hz, J_{P-H} = 11.5 Hz, 9H, (−OCH_3)$_3$), 2.76 (s, 1H, H_{endo}), 2.61 (s, 2H, H_1, H_4 (outer)).

Monitoring the Reduction of 8a by Low-Temperature ^{1}H NMR. A solution of **8a** (40 mg, 103.2 mol) in d_6-acetone, contained in a 5 mm NMR tube under argon, was cooled to −80 °C in an acetone/dry ice bath. In a separate 5 mm NMR tube a 3:1 excess (12 mg, 0.3 mmol) of $NaBH_4$ in d_6-acetone was cooled in the same bath. It was necessary to use an excess of hydride reagent, as the deuterated acetone was wet. After a 5 min period the hydride solution was transferred on top of the frozen solution of the cation. After a further 5 min, the NMR tube containing the mixture was upturned and immediately placed back in the bath. This procedure was repeated and the tube transferred to the probe of the instrument, held at −80 °C. ^{1}H NMR spectra were recorded in increments of 5 °C up to 20 °C.

Reduction of 13 using $NaBH_4$ and $NaBH_3CN$. The reduction of **13** was carried out in the same manner as that of **8a**. However, the ring adduct **15** eluted with petroleum ether (40−60 °C) and was easily separated from the hydride **14**, which was eluted with diethyl ether.

(η^5-C_5H_5)Fe(CO)(H)P(OEt)$_3$ (**14**): IR (cm^{-1}, acetone) ν(CO) 1945; ^{1}H NMR (δ, d_3−CD_3CN) 4.56 (s, 5H, C_5H_5), 3.91 (m, 6H, (−OCH_2−)$_3$), 1.21 (t, J_{H-H} = 5.9 Hz 9H, (−OCH$_2$CH_3)$_3$), −13.75 (d, J_{P-H} = 91.0 Hz, 1H, Fe*H*); ^{13}C NMR (δ, d_6-C_6D_6) 209.2 (d, J_{P-C} = 48.4 Hz, Fe*C*O), 79.9 (s, C_5H_5), 60.9 (d, J_{P-C} = 6.5 Hz, (−O*C*H$_2$−)$_3$), 16.4 (d, J_{P-C} = 7.9 Hz, (−O*C*H$_3$)$_3$); ^{31}P NMR (δ, d_3-CD_3CN) 181.3 (s, −*P*(OMe)$_3$). Anal. Calcd for $C_{12}H_{21}FeO_4P$: C, 45.60; H, 6.70; P, 9.81. Found: C, 45.12; H, 6.81; P, 9.70.

(η^4-C_5H_6)Fe(CO)$_2$P(OEt)$_3$ (**15**): IR (cm^{-1}, acetone) ν(CO) 1975, 1916; ^{1}H NMR (δ, d_6-C_6D_6) 5.31 (s, 2H, H_2, H_3 (inner)), 3.79 (m, 6H, (−OCH_2−)$_3$), 2.85 (d, J_{H-H} = 11.0 Hz, 1H, H_{endo}), 2.68 (s, 2H, H_1, H_4 (outer)), 2.40 (t, J_{P-H} = 10.2 Hz, J_{H-H} = 11.0 Hz, 1H, H_{exo}), 1.06 (t, J_{H-H} = 7.0 Hz, 9H, (−OCH_3)$_3$); ^{13}C

(34) Asirvatham, V. S.; Gruhn, N. E.; Lichtenberger, D. L.; Ashby, M. T. *Organometallics* **2000**, *19*, 2215.
(35) Schumann, H. *J. Organomet. Chem.* **1986**, *304*, 341.

NMR (δ, d_6-C_6D_6) 218.5 (d, $J_{P-C} = 21.5$ Hz, Fe*C*O), 83.7 (s, C_2, C_3), 60.3 (s, ($-OCH_2-$)$_3$), 50.8 (s, C_1, C_4) 45.2 (s, C_5), 16.2 (d, $J_{P-C} = 7.5$ Hz, ($-OCH_3$)$_3$); ^{31}P NMR (δ, d_6-C_6D_6) 193.1 (s, $-P$(OMe)$_3$). Anal. Calcd for $C_{13}H_{21}FeO_5P$: C, 45.38; H, 6.15; P, 9.00. Found: C, 45.11; H, 6.27; P, 8.72.

Calculational Methods. All calculations were carried out using the hybrid B3LYP functional, which has become the standard for studies of transition-metal-containing systems[20] using DFT and has been successfully used in studies on similar complexes.[36] The basis set used for iron was adapted from Huzinaga's Fe(14s8p5d) set.[37] This set was converted into an Fe(14s10p6d/14s6p5d) set with polarization functions (exponents 0.042 and 0.130) also due to Huzinaga. The basis set used for the ligand atoms was the 6-31G(d) set of Pople and co-workers.[38] This combined basis set is referred to as HUZ1 in this study. All of the calculations were carried out without symmetry constraints using redundant internal coordinates. However, as noted in the text, some geometrical constraints were introduced in the latter stages of the optimization procedure for the phosphite species. Each stationary point located for the phosphine system (minimum and transition state) was characterized by vibrational frequency analysis at the appropriate level, whereas no frequency analysis was carried out for the species resulting from hydride attack on **8**. The total energies of the phosphine species are corrected for the zero-point energy, whereas those of the phosphite species are not; however, it is expected that the relative energies will be unaffected by such an omission.[39] The geometries for the transition states were initially located using the PM3(tm) formalism, reoptimized at the B3LYP/3-21G* level and then finally optimized at the B3LYP/HUZ1 level. All of the DFT calculations were carried out using the Gaussian 94 package;[40] the PM3(tm) calculations were carried out using the SPARTAN package, version 5.0.3.[41]

Acknowledgment. Dr. David Hegarty is thanked for his expert assistance in the use of, and access to, the facilities of the Centre for High Performance Computing Applications (CHPCA), University College Dublin. We also thank a reviewer for helpful comments.

Supporting Information Available: A listing of the optimized structures of the 14 species **1**−**12**, **TS1**, and **TS2**, together with selected ^{1}H NMR spectra for the low-temperature reactions. This material is available free of charge via the Internet at http://pubs.acs.org.

OM0009740

(36) Frenking, G.; Wagener, T. Transition Metal Chemistry. In *Encyclopaedia of Computational Chemistry*; Schleyer, P. v. R., Ed.; Wiley: Chichester, U.K., 1998.

(37) Huzinaga, S. *Gaussian Basis Sets for Molecular Calculations*; Elsevier: New York, 1984; p 345.

(38) Ditchfield, R.; Hehre, W.J.; Pople, J. A. *J. Chem. Phys.* **1971**, *54*, 724. Hehre, W. J.; Ditchfield, R.; Pople, J. A. *J. Chem. Phys.* **1972**, *56*, 2257. Hariharan, P. C.; Pople, J. A. *Mol. Phys.* **1974**, *27*, 209. Gordon, M. S. *Chem. Phys. Lett.* **1980**, *26*, 163. Hariharan, P. C.; Pople, J. A. *Theor. Chim. Acta* **1973**, *28*, 213.

(39) Margi, P.; Deng, L.; Ziegler, T. *J. Am. Chem. Soc.* **1998**, *120*, 5517.

(40) Frisch, M. J.; Trucks, G. W.; Schlegel, H. B.; Scuseria, G. E.; Robb, M. A.; Cheeseman, J. R.; Zakrzewski, V. G.; Montgomery, J. A., Jr.; Stratmann, R. E.; Burant, J. C.; Dapprich, S.; Millam, J. M.; Daniels, A. D.; Kudin, K. N.; Strain, M. C.; Farkas, O.; Tomasi, J.; Barone, V.; Cossi, M.; Cammi, R.; Mennucci, B.; Pomelli, C.; Adamo, C.; Clifford, S.; Ochterski, J.; Petersson, G. A.; Ayala, P. Y.; Cui, Q.; Morokuma, K.; Malick, D. K.; Rabuck, A. D.; Raghavachari, K.; Foresman, J. B.; Cioslowski, J.; Ortiz, J. V.; Stefanov, B. B.; Liu, G.; Liashenko, A.; Piskorz, P.; Komaromi, I.; Gomperts, R.; Martin, R. L.; Fox, D. J.; Keith, T.; Al-Laham, M. A.; Peng, C. Y.; Nanayakkara, A.; Gonzalez, C.; Challacombe, M.; Gill, P. M. W.; Johnson, B. G.; Chen, W.; Wong, M. W.; Andres, J. L.; Head-Gordon, M.; Replogle, E. S.; Pople, J. A. *Gaussian 98*; Gaussian, Inc.: Pittsburgh, PA, 1998.

(41) SPARTAN, version 5.0.3; Wavefunction Inc., Irvine, CA, 1997.